THE ASTROPHYSICAL JOURNAL, 446:574–582, 1995 June 20

ARE NUCLEAR HOT SPOTS IN GALAXIES SITES OF SEQUENTIAL STAR FORMATION?

V. KORCHAGIN,[1] A. K. KEMBHAVI,[2] Y. D. MAYYA,[3] AND T. P. PRABHU[4]
Received 1994 July 18; accepted 1994 December 12

ABSTRACT

We investigate self-regulated propagation of star formation, which is one of the possible scenarios of star formation in molecular clouds fragmented into cold dense structures with masses lying near the Jeans limit. Strong ultraviolet (UV) radiation from newborn massive stars compresses nearby dense inhomogeneities, triggering further star formation. Once initiated, the star formation wave propagates with a velocity determined by the parameters of cloud inhomogeneities. The total UV flux increases as a result of continued star formation leading to enhanced heating and evaporation of protostellar inhomogeneities. Once the UV flux reaches a critical value, propagation of star formation has to stop. Thus the star formation in such a scenario has a built-in self-regulatory mechanism.

The nuclear *hot spots* in galaxies are explained here as sites of self-regulated star formation activity with the UV flux serving as the trigger and regulator. We determine theoretically an integral stellar spectrum for this scenario and compare it with the results for the instantaneous burst scenario. The observed optical colors and low equivalent widths of hot spots cannot be explained with an instantaneous burst, but agree well with self-regulated sequential star formation lasting for a few to several tens of million years.

Subject headings: galaxies: stellar content — stars: formation

1. INTRODUCTION

Observations accumulated over the last decade have demonstrated that a significant fraction of disk galaxies undergo starbursts in their nuclear and extranuclear regions. Starbursts can be triggered either by interactions with other galaxies which induce gas motions due to tidal forces, or due to internal dynamical processes which lead to a transport of gas to the central regions. The details of the processes which lead to starbursts are, however, quite unclear at the present time, and investigating the evolution of the star-forming nuclear regions is crucial to mitigate this ignorance.

In appearance and spatial extent the nuclear star-forming regions, known as *hot spots*, resemble giant extragalactic H II regions (GEHR) situated in the spiral arms and disks of galaxies, though their outer edges are more sharply bounded. Statistically, hot spots are redder in optical colors, but they are comparable in luminosity to the most luminous disk H II regions (Kennicutt, Keel, & Blaha 1989). The similarity noticed by these authors could be coincidental, but more probably it suggests that star-forming nuclear regions in spirals are governed by the same mechanisms that limit the scale of H II regions in the disk.

Observations reveal one important difference in the physical properties of hot spots and GEHRs: hot spots have lower Hα emission equivalent widths compared to GEHR's although the Hα luminosities are comparable (Kennicutt et al. 1989; Mayya 1994a). This implies a stronger continuum in the nuclear H II regions. Kennicutt et al. discussed two different possibilities for explaining the low equivalent widths of the hot spots. The first is a strong deficiency of high-mass stars in the stellar initial mass function (IMF), which, however, looks unrealistic since it would require too high a star formation rate in order to account for the observed amount of ionizing flux. The second, more plausible, explanation involves an accumulation of stars from many generations. This requires the star formation in the hot spots to take place over timescales that are much longer than those relevant to normal disk H II regions.

If a generation of stars triggers another one, and this process propagates over many generations in a particular star-forming region, an accumulation of stars evolved to different stages can naturally be produced. Although the idea of triggered and propagating star formation was formulated a long time ago (Öpik 1953; Hoyle 1953), there are only a few well-recognized observational examples of the phenomenon (Dopita, Mathewson, & Ford 1985; Wilding et al. 1993; Elmegreen 1992).

The present study is an attempt to understand whether the scenario of induced star formation could be used in the interpretation of optical data on the nuclear hot spots of galaxies.

2. FORMULATION OF THE MODEL

In this section we will describe a model of induced star formation in a clumpy medium, and then apply it in the following section to obtain color evolutionary diagrams of nuclear star-forming regions. The consideration of star formation in a cloudy medium includes many different physical processes and parameters which have to be taken into account. These are explained in detail here and some plausible approximations made in order to make the computations feasible.

2.1. *Propagation of Star Formation in a Clumpy Medium*

Recent observational data have demonstrated that molecular clouds are composed of numerous dense clumps, each occupying a small volume. Lee et al. (1986) found condensations lying along the edge of the bright central part of the H II region M42, with estimated mass per condensation $\sim 50\ M_\odot$. Observational evidence for the existence of dense clumps in molecular clouds was given by Chini et al. (1993). The 1300 μm mapping of the HH24 system in the Orion B region shows a strong source of dust emission which is interpreted as a cold gravita-

[1] Institute of Physics, Stachki 194, Rostov-on-Don, Russia.
[2] Inter-University Centre for Astronomy and Astrophysics, Pune, 411007, India.
[3] Tata Institute of Fundamental Research, Homi Bhabha Road, Bombay 400005, India.
[4] Indian Institute of Astrophysics, Bangalore 560034, India.

tionally unstable cloud fragment with mass ~ 36–$52\ M_\odot$.

Wilson & Johnston (1989) have found inhomogeneities in the Orion A region with mass in the interval ~ 1–$150\ M_\odot$. These authors suppose that the initial formation of stars in Orion A is a chance event, and that the radiation-driven implosion of nearby molecular gas leads to propagation of the star formtion throughout the region.

The luminosity-driven hydrodynamics of the interactions between young stars and molecular clouds has been discussed by many authors (see Tenorio-Tagle 1982; Elmegreen 1992; Franco 1993). The radiation from hot, luminous, massive stars ionizes the surrounding interclump gas and forms an expanding H II region. The ultraviolet (UV) radiation cannot, however, easily ionize dense and compact clumps. Assuming pressure equilibrium between a clump and the surrounding gas of an H II region, Elmegreen (1992) has estimated the time of ionization of a clump to be $\sim 10^7$ yr if its radius is ~ 0.1 pc. Thus the time of collapse of a clump located near a massive OB star is shorter than its ionization time.

The high pressure of young H II regions can influence inhomogeneities in another way, stimulating further star formation. The H II region surrounds and pinches off the small clumps and can compress some of them into unstable configurations which eventually form stars. This is a picture of a small-scale triggering of star formation according to the classification of Elmegreen (1992).

The radius of an H II region in a dense interclump gas is a few parsecs, and the time of propagation of an ionization front is a few $\times 10^5$ yr. For example, if the intercloud density is 10^3 cm^{-3} and the stellar photon output is $\sim 10^{49}$ s^{-1}, the mean lifetime of a compact H II region is $\sim 5 \times 10^5$ yr and its mean radius ~ 3 pc (Tenorio-Tagle 1982). So massive stars can affect inhomogeneities toward the formation of new stars in their vicinity up to a radius of a few parsecs.

The implosion of inhomogeneities by the high-pressure ionized gas of H II regions is not the only possible mechanism for triggering star formation. Klein et al. (1983) considered radiation-driven implosion of inhomogeneities embedded in molecular clouds. They found that radiation of two nearby O stars rapidly compresses an inhomogeneity of $84\ M_\odot$ to Jeans instability. Of this mass, $\sim 44\ M_\odot$ ionizes and expands away from the object, but the rest collapses during a few $\times 10^5$ yr. Klein et al. concluded that the radiation-driven implosion is a highly effective mechanism for forming additional stars within an OB subgroup. Recently Cammerer & Shchekinov (1994) have discussed the radiation-driven implosion as a regulating mechanism for star formation on a kiloparsec scale.

2.2. *Formation of New Clumps*

Another possibility for triggering star formation is the formation of new clumps in the expanding shells of supernova remnants. Here the gas, which is compressed in shells, relaxes through internal processes such as radiative cooling and eventually fragments and collapses under its own gravity. However, the gravitational fragmentation of expanding shells occurs a while after the beginning of expansion, when the surface density of the shell is sufficiently high. Elmegreen & Wang (1988) have found that significant gravitational fragmentation takes place on a timescale

$$t_{\rm shell} \approx \frac{46\ {\rm Myr}}{n^{1/2}} \left(\frac{\rho_0}{\rho_1}\right), \qquad (1)$$

where n is the atomic hydrogen density in units of cm^{-3} and ρ_0/ρ_1 is the density contrast between the shocked and ambient medium.

The dynamics of supernova remnants in high-density media has been discussed by Tenorio-Tagle et al. 1990. For the velocity of the shock after the formation of dense outer shell they obtain

$$V_{\rm shock} = 4600 E_{51}^{1/8} n_7^{1/4} \left(\frac{t}{t_{\rm sg}}\right) {\rm km\ s^{-1}}, \qquad (2)$$

where E_{51} is the energy released in the supernova explosion in units of 10^{51} ergs, n_7 is the density of ambient medium in units of 10^7 cm^{-3}, and $t_{\rm sg}$ is the time of formation of a dense outer shell, given by the expression

$$t_{\rm sg} = 230 E_{51}^{1/8} n_7^{-3/4}\ {\rm days}.$$

The expansion of the supernova remnant in the dense medium lasts until the moment when the shock velocity is comparable with the sound velocity in the ambient medium. Assuming that expansion occurs in an interclump medium with density $n_{\rm H_2} = 10^3$ cm^{-3} and thermal velocity 10 km s^{-1}, one can find from expression (2) that the expansion timescale of the supernova shell is $\sim 10^5$ yr. On the other hand, the gravitational fragmentation timescale for the assumed ambient density is about $\sim 10^6$ yr. Therefore, in dense media rapidly evolving supernova remnants do not reach the stage of gravitational fragmentation and formation of new clumps. However, supershells, produced by multi-supernova explosions, can evolve toward the stage of gravitational fragmentation. Numerical simulations, performed by Tenorio-Tagle et al. (1990), demonstrated the development of dense fragments resulting from shell instability about 30 Myr after the beginning of the expansion. The above estimates show that if new clumps can appear in the hot spots, they will appear at the last stages of their evolution. We therefore assume in our calculations that there is no new clump formation in star-forming regions.

2.3. *Self-regulating Mechanisms of Star Formation*

Star formation does not always stimulate further star-forming activity, and under some circumstances it can shut it off as well. On small scales, the mechanism for suppression of star formation which has been considered most thoroughly is the quick erosion of a molecular cloud by a hot massive star located near the cloud's external boundary (Tenorio-Tagle 1979; Whitworth 1979). The radiation from the star evaporates the cloud with a high mass-loss rate and as a result suppresses star formation. However, if the star cluster is born inside the cloud, the corresponding H II regions are compact, and the erosion is less efficient (Franco 1992).

The star formation in the circumnuclear region of a galaxy develops under conditions which make difficult the boundary erosion of the parent clouds. Observations show that the regions of the most recent star formation in the central region of galaxies are deeply buried in dense cloud complexes, revealing themselves only in nonthermal radio emission. It is therefore reasonable to suppose that "champagne flows" will be ineffective in the suppression of star formation in these regions. The much higher gas density in hot spots compared with the density in most disk H II regions (Kennicutt 1994) provides another observational hint that erosion is ineffective in the central regions.

We consider another mechanism which regulates star-forming activity inside dense molecular cloud complexes and determines the total number of stars, and eventually the size of a *miniburst* region. This is the photoevaporation of small clumps caused by the integral flux of radiation from newly born OB stars. The sequential star formation leads to an increase in the size of the star-forming region and to the consequent increase of the total mass of high-luminosity stars. The growing UV flux injected into the interstellar medium increases the rate of evaporation of inhomogeneities. When the evaporation time scale becomes less than the timescale for the collapse of inhomogeneities imploded by the radiation, the propagation of star formation stops and the later evolution of the region is determined by the evolution of the already existing stars.

A detailed investigation of the photoevaporation of inhomogeneities was recently carried out by Bertoldi & McKee (1990). They considered the quasi-stationary shape of photoevaporating inhomogeneities under the nonsymmetric radiation of a hot star. They found that photoevaporating clouds have a comet-like appearance, and the radiative mass loss in units of $M_\odot$ yr^{-1} is determined by the equation

$$\frac{dm}{dt} \sim -10^{-3}\left(\frac{S_{49}}{R_{\rm pc}^2}\right)^{1/2} r_{c,\rm pc}^{3/2} . \tag{3}$$

Here $S = S_{49} \times 10^{49}$ s^{-1} is the star's photon emission beyond the Lyman limit, $R_{\rm pc}$ is the distance in parsecs between the star and the inhomogeneity, and $r_{c,\rm pc}$ is the radius of inhomogeneity. We note that the rate of evaporation of clumps in a cometary stage differs significantly from the rate of evaporation of a clump symmetrically heated by radiation. Photoevaporation in a cometary phase is more effective because of the constant blowing away of the upper ionized layer of a clump.

Clumps in a star-forming cluster are affected by the integral ionizing radiation of stars, shining at different distances. The integral mass loss of a clump in a cometary phase can be estimated from equation (3) as

$$\frac{dm}{dt} \sim -10^{-3}\left(\frac{S_{49}N}{R_{\rm sf}^2}\right)^{1/2} M_\odot \ {\rm yr}^{-1} , \tag{4}$$

where N is the total number of massive stars in a cluster, and $R_{\rm sf}$ is a length scale of a star-forming region in parsecs.

We choose the mass of a typical clump to be 50 $M_\odot$ with a particle number density 10^4 cm^{-3}. Note that these values are close to the observational ones for bright-rimmed clouds around H II regions, possible candidates for star formation by radiation-driven implosion (Sugitani & Ogura 1994).

The time of collapse of such a clump is $\sim(G\rho)^{-1/2} \sim$ few $\times 10^5$ yr. Star formation in a cloud is suppressed if the evaporation time obtained using equation (4) is smaller than the collapse time. If the typical radius of a star-forming region is $\sim$100 pc, the critical UV photon flux which leads to such a time of evaporation and therefore to the suppression of star formation is $\sim$few $\times 10^{51}$ photons s^{-1}. The Lyman continuum luminosity of hot spots as estimated from Hα luminosity (assuming typical extinction $A_v = 1.5$) lies in the range 10^{51}–2×10^{52} photons s^{-1} (Kennicutt et al. 1989; Mayya 1994a). Thus in many hot spots it is sufficient to suppress further star formation, and might be forming stars in a regulated manner. It should be noticed, however, that the critical UV flux strongly depends on the density of inhomogeneities. If the density of inhomogeneities exceeds 10^5 cm^{-3}, the critical ionizing flux necessary to suppress star formation exceeds the typical values observed in hot spots. Therefore photoevaporation can effectively regulate star formation only for clump density less than 10^5 cm^{-3}.

2.4. *The Equations*

The most important properties of induced star formation are the nonlocal influence on the rate of star formation and the delay inherent in the response of a cloud to the influence. There are several possible mechanisms for stimulating star formation including ionizing radiation, stellar winds, and interstellar shocks (see Elmegreen 1992). All these mechanisms act inside some volume of characteristic size L. Inhomogeneities in the ISM, which are affected inside this *sphere of influence*, transform into a new generation of stars after a characteristic time T. These two parameters play a key role in the process of propagation of star formation. In particular, they determine the characteristic velocity of the process, which is

$$U_{\rm sf} \sim \frac{L}{T} .$$

The rate of induced formation of a new generation of stars at time t can be described by a propagation term of the form (Neukirch & Feitzinger 1988; Korchagin & Ryabtsev 1989)

$$kaM_c(x, t-T) \int {\rm d}x' f(x-x')M_s(x', t-T) . \tag{5}$$

Here M_c and M_s are the mass density of inhomogeneities and massive stars respectively, f is an *influence* function, describing the nonlocal interaction of massive stars at x' and clumps at x. We assume that the function f is spherically symmetric and $f = 0$ for $|x - x'| \geq L$. We assume for simplicity that $f =$ constant for $|x - x'| \leq L$ and is normalized to unity:

$$\int dx\, f(|x|) = 1 .$$

The coefficient a is the cross section for star-cloud interactions and the coefficient k determines the efficiency of the formation of stars from the cloud phase.

The set of equations describing mass exchange between the stars and clouds can now be written as

$$\frac{dM_s}{dt} = -D + kaM_c(x, t-T) \times \int dx' f(x-x')M_s(x', t-T) , \tag{6}$$

$$\frac{dM_c}{dt} = -aM_c(x, t) \int dx' f(x-x') \times M_s(x', t) - \Gamma M_c\, g\left(\int M_s\, dx\right) . \tag{7}$$

Equation (6) describes the process of birth of massive stars due to induced star formation and the decrease in the number of stars due to the death rate D. Equation (7) determines the rate of the decrease of cloud density due to the radiative influence of massive stars. Clumps irradiated by already existing stars with density M_s transform after time delay T into a new generation of stars. The last term on the right-hand side of equation (7) describes the self-regulating character of star formation, dis-

cussed in § 2.3, through the coefficient g. We assume that $g = 0$ for $M \leq M_{\rm crit}$ and $g = 1$ for $M > M_{\rm crit}$, where M is the total mass in stars and $M_{\rm crit}$ is the critical mass. When the total mass of stars exceeds the critical mass, there is evaporation of the clouds, inhibiting star formation. The diffusion coefficient Γ is described in § 2.5.

The development of propagating waves of star formation described by equations (6) and (7) has been discussed earlier (Neukirch & Feitzinger 1988; Korchagin & Rybtsev 1989, 1992). We are interested here in the color evolution of star-forming regions, and a generalization of equations (3) and (7) which takes into account the mass spectrum of the star-forming region is therefore necessary.

We follow common practice (see, e.g., Larson 1992) and assume that the IMF is a universal power law that does not vary with time or location. The number of stars formed per unit time as a function of mass is $\propto m^{-\alpha}$, with α a constant. Even in the stationary case where the power law is independent of time, the observed slope of the stellar mass distribution is different from α, because of the different timescale over which stars with different masses evolve.

In a nonstationary case the observed mass function becomes dependent on time. Using Equation (5) and the assumptions about the IMF that we have made, we can write

$$kaM_c(x, t-T)\int dx' f(x-x')M_s(x', t-T) = N_0(x, t-T)\int_{m_{\rm min}}^{m_{\rm max}} m^{1-\alpha}dm\,, \quad (8)$$

with each side of the equation indicating the rate of increase in the mass density of stars. Here $m_{\rm min}$ and $m_{\rm max}$ are the lower and the upper bounds on stellar masses in the burst. According to equation (8) the number of stars formed at time t per unit time, per unit volume in the mass interval $(m, m + dm)$ is

$$B(x, m) = \frac{(2-\alpha)m^{-\alpha}dm}{m_{\rm max}^{2-\alpha} - m_{\rm min}^{2-\alpha}}\, kaM_c(x, t-T) \times \int dx' f(x-x')M_s(x', t-T)\,. \quad (9)$$

At time t the number of star deaths per unit time in the mass interval $(m, m + dm)$ is

$$D(x, m) = -\frac{(2-\alpha)m^{-\alpha}dm}{m_{\rm max}^{2-\alpha} - m_{\rm max}^{2-\alpha}}\, kaM_c[x, t-T-\tau(m)] \times \int dx' f(x-x')Ms[x', t-T-\tau(m)]\,, \quad (10)$$

where $\tau(m)$ is the lifetime of a star of mass m. The equation describing the evolution of number density of stars having mass m can then be written as

$$\frac{dN(x, m)}{dt} = B(x, m) - D(x, m)\,. \quad (11)$$

To start the process of induced star formation as described by equations (6) and (7) we suppose that at some initial moment there spontaneously appears a stellar cluster with density distribution $M_{\rm so}(r)$. Then the rate of decrease of stellar mass density in equation (6) is given as the sum of death rate of stars in the initial cluster and the death rate of stars born as a result of nonlocal interaction:

$$D(r, t) = \int_{m_{\rm min}}^{m_{\rm max}} D(m)m dm + \frac{(2-\alpha)M_{\rm so}(r)}{m_{\rm max}^{2-\alpha} - m_{\rm min}^{2-\alpha}} \times \int_{m_{\rm min}}^{m_{\rm max}} m^{1-\alpha}\delta(t-\tau(m))dm\,. \quad (12)$$

2.5. *Diffusion Approximation*

The system of equations (6)–(12) can be simplified if the radius within which the inhomogeneities are influenced by nearby massive stars is much less than the size of the region of star formation. This assumption is a good approximation because, as mentioned above, the radius of influence of massive stars is ~ 1 pc, while the typical size of the star forming hot spots is $\sim 10^2$ pc.

As was shown by Neukirch & Feitzinger (1988) and Korchagin & Ryabtsev (1989), the propagation of star formation can in this case be described by a diffusion-like equation. Introducing a new variable of integration $x' - x = \xi$, and using a multiple Taylor expansion of the function $M_s(x', t-T)$ in a three-dimensional case, one can rewrite expression (5) in the form

$$aM_c(x, t-T) \times \left[M_s(x, t-T) + \tfrac{1}{6}\int_V d\xi f(|\xi|)|\xi|^2\nabla^2 M_s(x, t-T)\right], \quad (13)$$

where we have taken into account the normalization condition on the propagation function f and its spherical symmetry.

With help of equation (13), the system of equations (6)–(10) can be rewritten in a dimensionless form for a spherically symmetric wave of star formation as

$$\frac{\partial M_s}{\partial t} = -D + k\tilde{a}M_c(r, t-1)M_s(r, t-1) + 0.1L^2k\tilde{a}M_c(r, t-1)\frac{1}{r^2}\frac{\partial}{\partial r}\left[r^2\frac{\partial}{\partial r}M_s(r, t-1)\right], \quad (14)$$

$$\frac{\partial M_c}{\partial t} = -\tilde{a}M_c(r, t)M_s(r, t) - 0.1L^2\tilde{a}M_c(r, t) \times \frac{1}{r^2}\frac{\partial}{\partial r}\left[r^2\frac{\partial}{\partial r}M_s(r, t)\right] - \Gamma M_c(r, t)g\,, \quad (15)$$

$$B(m) = \frac{(2-\alpha)m^{-\alpha}}{m_{\rm max}^{2-\alpha} - m_{\rm min}^{2-\alpha}}\, k\tilde{a}M_c(r, t-1) \times \left\{M_s(r, t-1) + 0.1L^2\frac{1}{r^2}\frac{\partial}{\partial r}\left[r^2\frac{\partial}{\partial r}M_s(r, t-1)\right]\right\}, \quad (16)$$

and

$$D(m) = \frac{(2-\alpha)m^{-\alpha}}{m_{\rm max}^{2-\alpha} - m_{\rm min}^{2-\alpha}}\, k\tilde{a}M_c[r, t-1-\tau(m)] \times \left[\left[M_s[r, t-1-\tau(m)] + 0.1L^2\frac{1}{r^2} \times \frac{\partial}{\partial r}\left\{r^2\frac{\partial}{\partial r}M_s[r, t-1-\tau(m)]\right\}\right]\right]. \quad (17)$$

Here time is measured in units of the time delay T, density in units of unperturbed average density of a molecular cloud $M_{\rm co}$,

and length in parsecs. The dimensionless coefficients in the equations (14)–(17) have the form

$$\tilde{a} = aM_{co}\,T\,,$$
$$\tilde{\Gamma} = \Gamma T\,.$$

The diffusion terms in equations (14)–(15) describe the propagation of star formation. For our choice of parameters (see § 2.6), the velocity of propagation of a star-forming wave, as determined from numerical calculations, is ~ 2 km s^{-1}, which is in good agreement with theoretical estimates (Korchagin & Ryabtsev 1989). In ~ 70 M yr the star formation spreads over a distance of ~ 100 pc, involving much of the cloud material in the hot spot in the star-forming process.

2.6. *Parameters of the Model*

The main parameters determining the evolution of the stellar content in our model are those which define the IMF in the star-forming region, namely, the mass limits $m_{\min}$ and $m_{\max}$ and the slope of the IMF α. The two other key parameters of the model are the efficiency of star formation k and the dimensionless cross section of star-clump interactions $\tilde{a}$.

Recently Larson (1992) has discussed the nature of the IMF. He finds that presently available observational data as well as some theoretical arguments are consistent with the assumption that the IMF has the same basic form everywhere and can be characterized by a lower mass limit $\simeq 1 \times M_\odot$ with possibly a universal power law tail toward higher masses. We choose in our calculations the conventional IMF with slope $\alpha = 2.35$, and stellar mass intervals $1\,M_\odot \leq m_s \leq 30\,M_\odot$.

The star formation efficiency (SFE) is an important parameter of the theory. The estimations of SFE from observational data show that it varies in a very large range with the median value 0.02 (Myers et al. 1986). These authors noticed, however, that their approach can underestimate the SFE because it does not take into account the possible contribution of previous generations of stars in a star-forming region. Also, the theoretical estimates (see, e.g., Franco 1993) give higher values for the SFE, $\simeq 0.05$, and we choose this value in our calculations.

The cross section of star-clump interaction can be only roughly estimated. Assuming that all cloud material in a star-forming region is converted due to star-gas interactions, we can write, to order of magnitude,

$$\frac{M_c}{T_{\rm evol}} \sim \tilde{a} M_c M_s\,.$$

If the SFE is equal to 0.05 and the time of evolution of a star-forming region is a few $\times 10^7$ yr, the dimensionless coefficient $\tilde{a}$ is of the order of unity. We use in our calculations the value $\tilde{a} = 1.5$. As per the estimate in § 2.3, the critical UV photon flux which is required to suppress new star formation is $\sim 10^{52}$ photons s^{-1}. Such a flux beyond the Lyman continuum limit can be produced by a star cluster with total mass $1.3 \times 10^6\,M_\odot$, assuming the standard Salpeter IMF slope. We therefore choose in our calculations the value $M_{\rm crit} = 10^6\,M_\odot$.

The parameter $\tilde{\Gamma}$ determines the time of decay of clumps when the total mass of an association exceeds the critical value $M_{\rm crit}$. The decay time should be shorter than the time of gravitational collapse, and therefore $\tilde{\Gamma} > 1$. The value of $\tilde{\Gamma}$, however does not influence much the results of our calculations.

The lifetime $\tau(m)$ of stars in the nuclear phase was taken from Schaller et al. (1992). The time of delay T is determined by the time of development of H II regions around massive stars, which is $\sim 10^5$ yr, and by the collapse timescale for compressed clumps, which is $\sim 10^5$ yr. We therefore choose in our calculations $T = 5 \times 10^5$ yr.

2.7. *Synthesis of Observables*

Once the above set of equations is solved to obtain the number of stars as a function of mass and time, the total luminosity per unit mass is computed as

$$L_B(t) = \left(\frac{1}{M_T}\right) \sum_m \sum_\tau l_B(m, \tau) N(m, \tau, t)\,,$$

where $N(m, \tau, t)$ is the number of stars at time t with mass m and age τ, and $l_B(m, \tau)$ is the corresponding luminosity of the star in the B band. Here t is the time elapsed since the beginning of star formation; M_T is the total mass of the region in presently existing stars. We used $l_B(m, \tau)$ values from Mayya (1993, 1994b), which are based on new atmospheric models of Kurucz (1992). The methods followed in these computations are briefly described below. Stellar evolutionary models of Schaller et al. (1992) were used first to obtain $T_{\rm eff}$ and log (g) for a range of masses at time intervals of 0.2 Myr. Kurucz (1992) atmosphere models were then used to assign a spectrum for each set of $T_{\rm eff}$ and log g at all 1221 Kurucz wavelength points from 22.8 to 160,000 nm. The resultant spectrum was integrated over the *BV RI J H K L M* bands to get the luminosities. Additionally, Lyman continuum and helium continuum luminosities were obtained by integrating the spectra shortward of 91.2 and 50.4 nm respectively. The new Kurucz models are available for $3500 \leq T_{\rm eff} \leq 50{,}000$. For the range of masses considered in the present study, $T_{\rm eff}$ remained lower than 50,000 K. During red supergiant phases of some massive stars (for $m < 20$ at ages > 10 Myr), $T_{\rm eff}$ falls below 3500 for short timescales, in which case $T_{\rm eff}$ is forced to 3500 K. This approximation may affect the computations in the near-infrared region (e.g., K band), but its effect on optical and ultraviolet regions is negligible. The computed Lyman continuum photon luminosity was used for obtaining the expected Hβ luminosity ϕ from a gaseous nebula at 10,000 K (Osterbrock 1989),

$$\phi = 4.78 \times 10^{-13}\,N_L\,.$$

We use in our calculations the ratio ϕ/L_B, which is similar to equivalent width of Hβ, but is more easily obtained from imaging observations. The model results were compared with other similar models in the literature for conventional scenarios of star formation, and the agreement was found to be very good with Mas-Hesse & Kunth (1991).

The results of computations for sequential star formtion are given in Table 1. The age in the first column is the time elapsed since the beginning of the star formation, and the following four columns describe the evolution of observable parameters log (ϕ/L_B), $B-V$, $V-R$, and $V-K$. The last column gives the accumulated mass in all stars. An initial mass of $10^5\,M_\odot$ is assumed in the computations. For comparison, results of a model where all the stars are produced over a short timescale ("instantaneous burst") are also given in the second part of the table, with the computations based on Mayya (1994b). The two computations assume a Salpeter slope ($\alpha = 2.35$) for the IMF, with $1 \leq M/M_\odot \leq 30$. Figures 1*a*–1*d* show the behavior of various observable quantities. We have divided the mass range 1–30 $M_\odot$ into three bins with low ($M \leq 5\,M_\odot$), intermediate ($5 < M < 15\,M_\odot$), and high ($M \geq 15\,M_\odot$) mass stars. The fractional mass in each bin, including the initial stars as well as

TABLE 1

SEQUENTIAL STAR FORMATION COMPUTATIONS

Age	log (ϕ/L_b)	$B-V$	$V-R$	$V-K$	log (Mass)
A. Induced Star Formation Model					
0.20.....	−1.01	−0.23	−0.10	−0.65	4.99
2.00.....	−1.06	−0.23	−0.10	−0.67	5.01
4.00.....	−1.15	−0.24	−0.10	−0.70	5.03
6.00.....	−1.83	0.11	0.16	1.03	5.06
8.00.....	−1.74	0.28	0.43	2.90	5.09
10.00.....	−1.69	0.01	0.22	2.65	5.12
12.00.....	−1.60	0.01	0.21	2.68	5.15
14.00.....	−1.69	0.20	0.22	1.16	5.19
20.00.....	−1.53	0.02	0.20	2.40	5.29
30.00.....	−1.57	0.00	0.17	2.20	5.50
40.00.....	−1.69	0.08	0.20	2.07	5.71
50.00.....	−1.66	0.07	0.20	2.13	5.91
60.00.....	−1.72	0.08	0.20	2.13	6.09
69.00.....	−1.84	0.08	0.20	2.12	6.21
80.00.....	−3.75	0.05	0.14	1.90	6.18
B. Instantaneous Star Formation Model					
0.10.....	−1.00	−0.23	−0.10	−0.68	
2.00.....	−1.06	−0.24	−0.10	−0.70	
4.00.....	−1.16	−0.24	−0.11	−0.73	
5.00.....	−1.36	−0.24	−0.11	−0.74	
5.50.....	−1.51	−0.24	−0.11	−0.75	
6.00.....	−1.83	0.17	0.20	1.17	
6.50.....	−2.06	0.40	0.34	1.84	
7.00.....	−2.03	0.19	0.26	1.74	
8.00.....	−2.24	0.14	0.30	2.40	
9.00.....	−2.47	0.15	0.31	2.76	
10.00.....	−2.64	0.24	0.36	3.17	
12.00.....	−2.96	0.25	0.33	3.36	
14.00.....	−3.34	0.28	0.21	2.61	
16.00.....	−3.68	0.12	0.11	2.79	
18.00.....	−3.68	0.33	0.22	3.37	
20.00.....	−3.85	0.33	0.19	3.32	

NOTES.—Initial mass function parameters used are M(low) = 1, M(up) = 30, slope = 2.35. Solar metallicities are used.

those formed due to the trigger, is shown as a function of the time t by appropriately marked curves in Figure 1*a*. As expected, the low-mass stars contribute to the total mass at all times. The fractional contribution of the Lyman continuum luminosity for the three mass ranges is shown in Figure 1*b*. The contribution mainly comes from massive stars, until such time when the total UV flux suppresses further star formation, which happens after 70 Myr. Thereafter the highest surviving masses contribute to the total ionizing luminosity. The fractional contributions in the optical bands B and R are plotted in Figure 1*c* and 1*d* respectively. As can be seen, it is the intermediate- and low-mass stars which dominate the optical luminosity at all times after about 10 Myr. The peaks between 10 and 20 Myr are due to the red supergiant phases of the stars formed initially ($t = 0$).

At the beginning of the process the fractional contribution of newborn stars is low, and therefore the process is qualitatively similar to an instantaneous burst of star formation. As a result, the colors become red ($B-V = 0.10$–0.28) at 6–8 Myr. The color turns slightly bluer thereafter, because of the increasing fraction of newly formed stars. For example, the number of stars formed due to the trigger equals the initial number of stars in about 20 Myr. The Hβ equivalent width, or equivalently [log (ϕ/L_B)], reaches a steady state value after 10 Myr, lasting up to 70 Myr, when the regulation mechanism suppresses further star formation. After the suppression the color evolution of a star-forming region is determined by the rate of death of massive stars, rapidly decreasing the Hβ equivalent width. The "steady phase" is absent in the instantaneous star formation scenario.

The key process determining the color evolution of a star-forming region is the induced star formation; the initial conditions do not have much influence on the outcome. This process plays a significant role when the mass of newborn stars become comparable with the initial mass of stars. As can be seen from equation (6), the time required for this is mainly determined by the coefficient of star-cloud interactions a, and the efficiency of star formation k.

3. RESULTS

3.1. *Data on Hot Spots*

Kennicutt et al. (1989) have compared the Balmer equivalent widths derived from CCD images in nuclear H II regions, hot spots, and disk H II regions. Recently, Mayya (1994a) has published a uniform set of optical photometric data on nuclear hot spots in galaxies NGC 1365, 2903, and 3351, along with a large number of disk H II regions. These data were obtained by CCD imaging in BVR and Hα bands. In both the studies, the aperture photometry was used to extract fluxes from hot spots, with care taken to subtract the strong bulge background accurately. Both the studies infer relatively lower Balmer equivalent width toward the nuclear hot spots, compared to disk H II regions. The availability of BVR photometry in addition to Hα flux in Mayya (1994a) makes this data ideal for the investigation of star formation histories in hot spots. We use the latter photometry for the study here.

From the tabulated BVR magnitudes and Hα fluxes, we derived log (ϕ/L_B). This requires knowledge of the extinction toward individual regions. Similarly the conversion of observed colors into extinction-free $B-V$ and $V-R$ colors also requires the knowledge of reddening. Presently only a few reddening measurements toward hot spots are available. Kennicutt et al. (1989) find more or less similar distributions of visual extinction toward disk H II regions and H II region nuclei, with most regions having extinction A_v between 1 and 2 mag. We assume that the hot spots also have similar extinction properties and use a value of $A_v = 1.5$ uniformly for all the regions. The resulting values are shown in Figures 2 and 3 for the three galaxies mentioned above. Figure 2 shows the observed points in ϕ/L_B vs. $B-V$ plane and Figure 3 shows them in $V-R$ vs. $B-V$ plane. The locus of points for a cluster evolving after an instantaneous burst is shown up to 20 Myr by the dotted line. The thick line is the expected track for a region with sequential star formation up to 80 Myr. In each figure the median values of the observables before and after correcting for extinction are denoted by filled inverted triangles and squares, respectively.

3.2. *Color Evolution of Hot Spots*

Comparison with the scenario of an instantaneous burst of star formation (Table 1) shows that observed values of log (Hβ/L_B) vs. $B-V$ for hot spots can be achieved after 6 Myr. This phase lasts only a very short time (2–3 Myr). We should assume therefore that all hot spots are observed during a very short period in their evolution. On the contrary, in the sequential star formation scenario, colors stay in the observed range for a few to several tens of Myr. Thus the observed red optical colors and low equivalent widths of hot spots can be explained

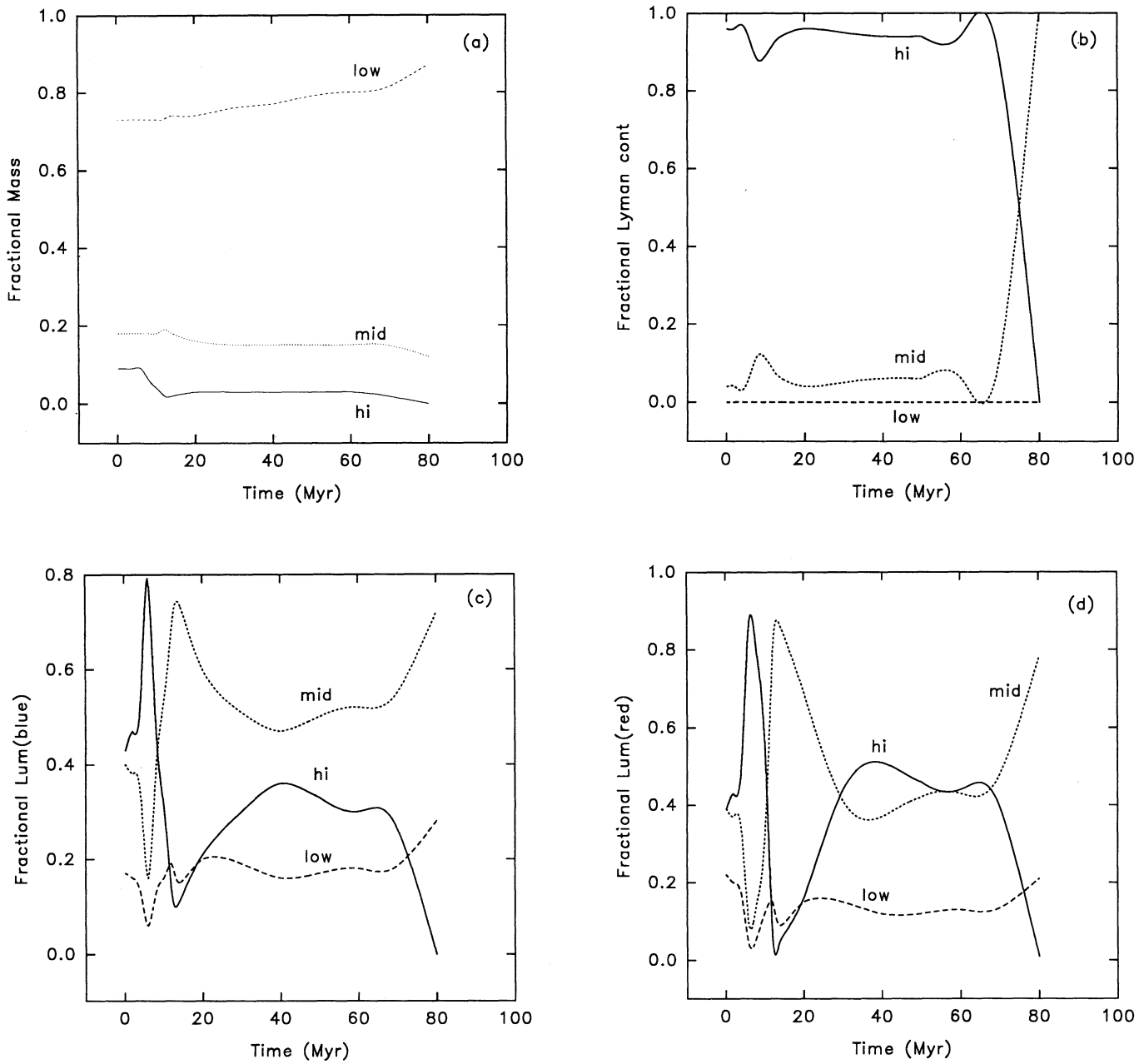

FIG. 1.—Fractional contributions from low—($m < 5$), intermediate—($5 < m < 15$), and high—($m > 15$) mass stars are plotted as a function of time elapsed since the star formation started. (*a*) Fraction of mass contributed by the three mass ranges, (*b*) Lyman continuum, (*c*) blue band, and (*d*) red band luminosity fractions.

as being due to sequential star formation with ages between 10 and 70 Myr.

The sequential star formation we have discussed above of course represents one of many possible scenarios for prolonged star formation in hot spots. However, it may be noted that according to recent observational data (Sugutani & Ogura 1994), a considerable number of stars in clumpy molecular clouds are formed by induced star formation through radiation-driven implosion of clumps. If OB stars are formed by this mechanism, the cutoff of star formation should be inevitable, and naturally explains the existence of observational points with low equivalent width in Figure 2. Based on these observational data and the theoretical models, we conclude that a highly plausible model of star formation in hot spots is one with sequential nature, lasting for a few to several tens of million years, until the *fuel* for further star formation is destroyed by the integral luminosity of massive UV stars. However, firm conclusions about the nature of star formation in hot spots will require further observational data.

4. DISCUSSION

Wynn-Williams & Becklin (1985) proposed a physical model to explain the distribution and appearance of hot spots. They suggested that the star formation takes place at locations spread over the central 600 pc in galaxy NGC 2903. The visual appearance of the central parts of NGC 2903 is then mainly a result of patchy foreground extinction and does not reflect real variations in stellar population and density. Simons et al.

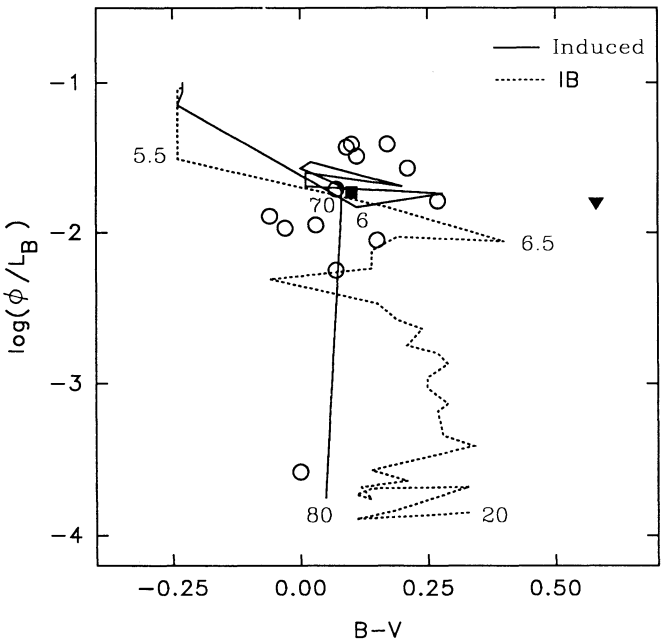

FIG. 2.—Observed quantities for hot spots (*open circles*), after correcting for typical extinction of $A_v = 1.5$ mag, are plotted in log (ϕ/L_B) vs. $B-V$ plane. The median of the observed quantities before and after extinction correction are denoted by a filled inverted triangle and square, respectively. The solid curve is the locus of points for sequential star formation up to 80 Myr. The dotted curve represents evolution of a cluster with an instantaneous burst of star formation up to 20 Myr. The observed values lie in the age range 6–70 Myr for sequential star formation or 6–8 Myr for an instantaneous burst. Salpeter's IMF with lower and upper cutoff masses 1 and 30, respectively, are used.

(1988), using infrared array imaging of the galaxy NGC 2903, came to a similar conclusion that hot spots can be better described as holes in the nuclear dust distribution in an extended volume of active star formation. But there is much direct and indirect evidence to show that star formation is distributed inhomogeneously in the central parts of the starburst galaxies. Probably the most important support for this point of view comes from the distribution of the nonthermal radio luminosity. Radio maps with high spatial resolution of the central region of NGC 1808 (Saikia et al. 1990) reveal a family of compact sources. The energetics and the indications of steep radio spectra strongly suggest that the compact radio sources are young SNRs. Compact radio sources are not directly associated with H II regions (Saikia et al. 1990; Forbes, Boisson, & Ward 1992), showing that regions of active star formation are distributed quite inhomogeneously within the nuclear regions. Star formation in circumnuclear regions of galaxies can be described as a set of minibursts, prolonged in time, embedded in a distribution of gas and dust complexes, surrounding the centers of galaxies. Each of these bursts is currently seen at a different stage of evolution. In evolved burst regions, most of the obscuring material surrounding the cluster of young stars is blown away by the radiation of massive OB stars, and the cluster appears as an optical hot spot.

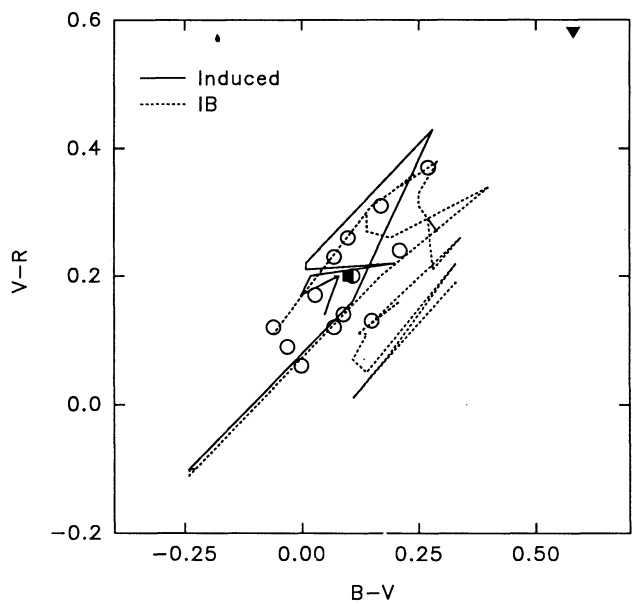

FIG. 3.—Same as Fig. 2, but with $V-R$ plotted vs. $B-V$. The ages inferred from Fig. 2 are consistent with this plot as well.

The spatial distribution of hot spots, which are often seen to be ordered in chains or rings, very likely reflects the large-scale dynamics of circumnuclear regions of galaxies. There are some strong observational evidences in support of this point of view. According to Kennicutt (1994), the circumnuclear "hot spot" star formation regions are probably the most distinctive signatures of bar-induced activity. Excess star formation is observed in 30%–50% of barred systems. Recent observations of CO and Hα distribution in nearby barred galaxies (Kenney et al. 1992) revealed that CO emission, arising mainly from *twin peaks* located symmetrically about the nucleus, coincides with elliptical rings of H II regions. Roy & Belley (1993) found a striking coincidence of a chain of H II regions with the molecular bar in the center of NGC 6946. These data indicate that the dynamical effects play a major role in the spatial distribution of hot spots. However, an intermediate-scale triggering, that is, pushing away and compressing of ambient gas into layers and stimulating further formation of new generations of hot spots also cannot be excluded. There are some observations of intermediate scale triggering in our own galaxy (Elmegreen 1992), but there is no observed example in circumnuclear regions of other galaxies.

The size of starburst knots in our model is determined by the velocity of propagation of star formation, and the duration of the process. For our choice of parameters, the velocity of a star-forming wave is ~ 2 km s^{-1}. If the duration of the process is ~ 60 Myr, the size of a starburst knot is about 200 pc. Observationally, hot spots have sizes ranging between 100 and 800 pc (Kennicutt et al 1989). The sequential star formation scenario can explain the "low-size wing" in the size distribution of hot spots in galaxies. These sizes are comparable with sizes of Brγ knots in NGC 1808 (Krabbe, Sternberg, & Genzel 1994). These authors concluded that Brγ knots coinciding with discrete radio sources are the actual sites of star-forming activity, while the optical hot spots are mainly the directions of low foreground extinction. Note, however, that strong ordering of giant hot spots in some galaxies cannot be coincidental and reflects the large-scale dynamical processes in galaxies. One possible explanation of the origin of ordered hot spots as a result of gravitational instability in the inner Lindblad resonance region of galaxies was recently proposed by Elmegreen (1994).

The detailed picture of star-forming activity in central regions of galaxies can be understood by considering gravitational and radiational hydrodynamical processes together.

5. CONCLUSIONS

In a model of nuclear starbursts in which the star formation progressively propagates in space and time, the star formation is found to regulate itself between 10 and 70 Myr. The observed quantities for hot spots in the nuclear regions of galaxies, especially the low Balmer emission line equivalent widths, are close to the regulated values. Thus, the hot spots differ from the disk H II regions mainly in the long duration of star formation.

The authors would like to thank an anonymous referee for very useful comments and suggestions.

REFERENCES

Bertoldi, F., & McKee, G. F. 1990, ApJ, 354, 529
Cammerer, M., & Scshekinov, Yu. 1994, A&A, 283, 845
Chini, R., Krugel, E., Haslam, C. G. T., Kreysa, E., Lemke, R., Reipurth, B., Sievers, A., & Ward-Thompson, D. 1993, A&A, 272, L5
Dopita, M. A., Mathewson, D. S., & Ford, V. L. 1985, ApJ, 297, 599
Elmegreen, B. G. 1992, in Star Formation in Stellar Systems, ed. G. Tenirio-Tagle, M. Prieto, & F. Sanches (Cambridge: Cambridge Univ. Press), 383
———. 1994, ApJ, 425, L73
Elmegreen, B. G., & Wang, M. 1988, in Molecular Clouds in the Milky Way and External Galaxies, ed. R. L. Dickman, R. L. Snell, & J. S. Young (Berlin: Springer), 240
Forbes, D. A., Boisson, C., & Ward, M. J. 1992, MNRAS, 259, 293
Franco, J. 1992, in Star Formation in Stellar Systems, ed. G. Tenorio-Tagle, M. Prieto, & F. Sanchez (Cambridge: Cambridge Univ. Press), 515
———. 1993, Rev. Mexicana Astron. Astrof., 26, 13
Hoyle, F. 1953, ApJ, 118, 513
Kenney, J. D. P., Wilson, C. D., Scoville, N. Z., Devereux, N. A., & Young, J. S. 1992, ApJ, 395, L79
Kennicutt, R. C. 1994, in Mass-Transfer Induced Activity in Galaxies, ed. I. Shlosman (Cambridge: Cambridge Univ. Press), 131
Kennicutt, R. C., Keel, W. C., & Blaha, C. A. 1989, AJ, 97, 1022
Klein, R. I., Maxwell, T., Sandford, M. T., II, & Whitaker, R. W. 1983, ApJ, 271, L6
Korchagin, V. I., & Ryabtsev, A. D. 1989, Ap&SS, 161, 321
———. 1992, MNRAS, 255, 19
Krabbe, A., Sternberg, A., & Genzel, R. 1994, ApJ, 425, 72
Kurucz, R. L. 1992, in IAU Symp. 149, Stellar Populations of Galaxies, ed. B. Barbuy & A. Renzini (Dordrecht: Kluwer), 225.
Larson, R. B. 1992, in Star Formation in Stellar Systems, ed. G. Tenorio-Tagle, M. Prieto, & F. Sanchez (Cambridge: Cambridge Univ. Press), 127
Lee, G. M., Scoville, N. Z., Baath, L. B., Masson, C. R., & Woody, D. P. 1986, ApJ, 304, L51
Mas-Hesse, J. M., & Kunth, D. 1991, A&AS, 88, 399
Mayya, Y. D. 1993, Ph.D. thesis, Indian Institute of Science, Bangalore
———. 1994a, AJ, 108, 1276
———. 1994b, MNRAS, submitted
Myers, P. C., Dame, T. M., Thaddeus, P., Cohen, R. S., Silverberg, R. F., Dwek, E., & Hauset, M. G. 1986, ApJ, 301, 398
Neukirch, T., & Feitzinger, J. V. 1988, MNRAS, 235, 1343
Öpik, E. J. 1953, Irish Astron. J., 2, 219
Osterbrock, D. 1989, Astrophysics of Gaseous Nebulae and Active Galactic Nuclei (Mill Valley: University Science Books)
Roy, J.-R., & Belley, J. 1993, ApJ, 406, 60
Saikia, D. J., Unger, S. W., Pedlar, A., Yates, G. J., Axon, D. J., Wolstencroft, R. D., Taylor, K., & Guldenkerne, K. 1990, MNRAS, 245, 397
Simons, D. A., DePoy, D. L., Becklin, E. E., Capps, R. W., Hodapp, K.-W., & Hall, D. N. B. 1988, ApJ, 335, 126
Schaller, G., Schaerer, D., Meynet, G., & Maeder, G., & Maeder, A. 1992, A&AS, 96, 269
Sugitani, K., & Ogura, K. 1994, ApJS, 92, 163
Tenorio-Tagle, G. 1979, A&A, 71, 59
———. 1982, in Regions of Recent Star Formation, ed. R. Roger & P. Dewdney (Dordrecht: Reidel), 1
Tenorio-Tagle, G., Rozyczka, M., & Bodenheimer, P. 1990, A&A, 237, 207
Whitworth, A. 1979, MNRAS, 186, 59
Wilding, T., Alexander, P., Crane, P., & Pooley, G. 1993, in Star Formation Galaxies and the Interstellar Medium, ed. J. Franco, F. Ferrini, & G. Tenorio-Tagle (Cambridge: Cambridge Univ. Press), 301
Wilson, T. L., & Johnston, K. J. 1989, ApJ, 340, 894
Wynn-Williams, C. G., & Becklin, E. E. 1985, ApJ, 290, 108